Impact of shipping emissions on air pollution and pollutant deposition over the Barents Sea

Jean-Christophe Raut, Kathy S. Law, Tatsuo Onishi, Nikos Daskalakis, Louis Marelle

Impact of shipping emissions on air pollution and pollutant deposition over the Barents Sea

Jean-Christophe Raut[a,*], Kathy S. Law[a], Tatsuo Onishi[a], Nikos Daskalakis[b], Louis Marelle[a]

[a] *Laboratoire, Atmosphères, Observations Spatiales (LATMOS)/IPSL, Sorbonne Université, UVSQ, CNRS, Paris, France*
[b] *Laboratory for Modeling and Observation of the Earth System (LAMOS), Institute of Environmental Physics (IUP), University of Bremen, Bremen, Germany*

Abstract

Arctic warming leading to reduced summertime sea-ice is likely to lead to increased local shipping especially along the Northeast Passage near the northern coasts of Norway and Russia, which are shorter than the traditional southerly routes. Here, the regional chemistry-transport model WRF-Chem is used to examine the effects of shipping emissions on levels of air pollutants and deposition fluxes over the Barents Sea both for present-day and future conditions, based on a high growth scenario. Present-day shipping emissions are found to have already substantial effects on ozone concentrations, but limited effects on sulphate and nitrate aerosols. Predicted future changes in ozone are also important, particularly in regions with low nitrogen oxide concentrations, and results are sensitive to the way in which diversion shipping is distributed due to non-linear effects on photochemical ozone production. Whilst modest future increases in sulphate and nitrate aerosols are predicted,

*Corresponding author
Email address: Jean-Christophe.Raut@latmos.ipsl.fr (Jean-Christophe Raut)
URL: http://raut.page.latmos.ipsl.fr/ (Jean-Christophe Raut)

large enhancements in dry deposition of sulphur dioxide and wet deposition of nitrogen compounds to the Barents Sea are predicted. Such levels of future nitrogen deposition would represent a significant atmospheric source of oceanic nitrogen affecting sensitive marine ecosystems.

Keywords: Future shipping diversion routes, Regional chemistry-transport model, Aerosol deposition, Barents Sea

---

1. Introduction

The Arctic region is undergoing unprecedented warming leading to reductions in summer sea-ice extent (Box et al., 2019; Pörtner et al., 2019). This is opening up the possibility for increased Arctic shipping notably along the Northeast Passage, extending from the north coast of Norway along the north coast of Russia. As sea-ice declines further shipping may also increase along the Northwest Passage traversing northern Canada and the north coast of Alaska or even across the Arctic Ocean (Melia et al., 2016; Stephenson et al., 2018). Projections underline large changes in the duration of the ship-accessible season across the Canadian Arctic (Mudryk et al., 2021). Arctic warming may also lead to increased industrial activities, such as oil and gas extraction, with associated port development, urbanisation and shipping (Dalsøren et al., 2007; AACA, 2017; Schmale et al., 2018). Such development will likely increase the footprint of local anthropogenic emissions, including shipping, relative to pollutants transported from midlatitudes (Marelle et al., 2018). Shipping emissions are known to emit nitrogen oxides (NO_x) and volatile organic compounds (VOCs) producing ozone (O_3) and emissions of precursor trace gases (sulphur dioxide SO_2, NO_x, VOCs) produc-

ing secondary aerosols, notably sulphate (SO_4^{2-}), nitrate (NO_3^-) and ammonium (NH_4^+), while black carbon (BC) is emitted directly (Corbett et al., 2010; Winther et al., 2014). Studies examining the effects of present-day shipping found substantial contributions to O_3 and fine particulate matter ($PM_{2.5}$, aerodynamic diameter less than 2.5μm) concentrations, exceeding background levels in and around shipping lanes, for example, along the Norwegian coast (Marelle et al., 2016), in the Baltic Sea (Jonson et al., 2015; Karl et al., 2019b) and along the Canadian Northwest Passage (Aliabadi et al., 2016; Gong et al., 2018) as well as enhanced aerosols from cruise shipping in Svalbard (Eckhardt et al., 2015) during the summer months. In common with air pollutants from other sources, ozone and $PM_{2.5}$ from shipping emissions can be harmful to human health causing chronic (e.g. respiratory and cardiovascular) disease and premature death (Im et al., 2018) even at low concentrations. Deposition of highly soluble pollutants containing acidic sulphur and nitrogen compounds can be damaging to vegetation and water bodies (lakes, oceans) and marine ecosystems. Nitrogen deposition can also lead to eutrophication and may affect the marine nitrogen cycle since nitrogen is a limiting nutrient for oceanic net primary productivity (NPP) (Duce et al., 2008; Randelhoff et al., 2020). While a recent study suggests, that atmospheric deposition to the Arctic ocean is not important compared to other fluxes (e.g. from rivers, coastal erosion) (Terhaar et al., 2021), it remains poorly quantified and may lead to enhanced NPP (Mills et al., 2018).

In the future, shipping along ice free Arctic routes is likely to increase. In particular, increased diversion of shipping from longer southerly routes along the shorter Northeast Passage, may increase local shipping emissions

and increase air pollution, both locally and regionally (Granier et al., 2006; Winther et al., 2014). Modelling studies estimated that critical loads could be exceeded along the coast of Norway (Dalsøren et al., 2007) whereas over the Baltic Sea nitrogen deposition is likely to be reduced following the introduction of a Nitrogen Emission Control Area (NECA) in 2021 (Karl et al., 2019a). Hassellöv et al. (2013) suggested that acidic pollutants emitted from shipping may contribute to regional pH reductions of the same order of magnitude as those due to carbon dioxide (CO_2) in regions with dense shipping traffic.

In this study, we focus on a region located north of Norway and Russia, centered over the Barents Sea, but also including parts of neighboring seas (Norwegian and Kara) and their coastal surroundings. This region is traversed by international shipping travelling from Europe to Russia and Asia along the Northeast Passage as well as local (fishing, cruise, passenger) shipping (Silber and Adams, 2019) and where increased future traffic is predicted (Corbett et al., 2010; Winther et al., 2014). There is also a high rate of marine productivity with substantial fishing stocks in this region as well as large natural resources, such as oil and gas (AACA, 2017). Here, we examine the impact of present-day and future shipping on atmospheric composition and deposition of trace gases and aerosols in the Barents Sea region with potential implications for human health and local ecosystems (Smedsrud et al., 2013). We used the regional WRF-Chem model (Section 2.1) run with present-day emissions and a high growth shipping scenario (Sections 2.2 and 2.3) to examine the potential future shipping impacts. Present-day and future scenario model results are discussed in terms of impacts on concentrations and depo-

sition (Section 3) before providing concluding remarks (Section 4).

2. Experiment setup - model simulations

2.1. Model setup

For this work we used the regional Weather Research and Forecasting model with Chemistry (WRF-Chem) (Fast et al., 2006; Grell et al., 2005). We use the version 3.5.1 including updates described in Marelle et al. (2017) which has also been used to study Arctic atmospheric composition and climate effects (Marelle et al., 2015, 2016; Raut et al., 2017; Marelle et al., 2018). Details about the WRF-Chem model setup including boundary layer physics, radiation and surface schemes are provided in Raut et al. (2017); Marelle et al. (2018). In particular, this model version was evaluated against atmospheric composition observations in Marelle et al. (2017) and used to investigate the contribution of remote and local sources of pollutants, including shipping emissions, to Arctic aerosols and their climate impact (Marelle et al., 2018).

In order to estimate the impact of Arctic shipping in the Barents Sea region, the model was run on a parent domain covering a large part of the Northern Hemisphere with a horizontal resolution of 100×100 km^2 and, via a one-way nest, over a region covering the Barents Sea and part of the Kara Sea, north of Norway and Russia with 20×20 km^2 horizontal resolution (Fig. .1). Fifty vertical levels were used in both domains. The model was run from March to August for the present-day (year 2012) and the future (year 2050). In each case, the first 3 months were considered as spin-up and were not used in the analysis.

[Figure 1 about here.]

2.2. Emissions

The model was run with the same emissions as Marelle et al. (2018) since, as noted above, it was thoroughly validated and improved in terms of simulating Arctic atmospheric composition (Marelle et al., 2017). This includes ECLIPSEv5 (Evaluating the Climate and Air-Quality Impacts of Short-Lived Pollutants, version 5) anthropogenic emissions (Stohl et al., 2015; Klimont et al., 2017) and hourly wild fire emissions from the NCAR Fire Inventory (FINNv1)(Wiedinmyer et al., 2011; Jiang et al., 2012). Biogenic emissions were calculated online using MEGAN (Model of Emissions of Gases and Aerosols from Nature)(Guenther et al., 2006).

Shipping emissions below 60°N were taken from the Representative Concentration Pathways (RCP8.5) dataset (van Vuuren et al., 2011) used in ECLIPSEv5b. At latitudes above 60°N, shipping emissions from the Arctic-wide Winther et al. (2014) inventory based on activity data from real-time satellite Automatic Identification System (AIS) ship positioning data for 2012 (Jalkanen et al., 2012) were used. Nunes et al. (2017) note that the use of AIS data for reporting activities and movements of ships is the best current approach. Winther et al. (2014) also included an evaluation of present-day and future evolution in engine efficiency and took into account new sulfur fuel regulations (Jonson et al., 2015). Emissions from Winther et al. (2014) are higher compared to previous Arctic shipping inventories such as Corbett et al. (2010). This is because, for example, this more recent inventory includes emissions from fishing ships which represent close to 40% of Arctic

shipping emissions Marelle et al. (2016), and because marine traffic was larger in 2012 than in the past. More recent shipping inventories are now available, including updated emissions in Winther et al. (2017) based on 2012-2016 AIS data, and ECLIPSEv6b based on STEAM3 emissions using 2015 AIS data, as described in Johansson et al. (2017). However, ECLIPSEv6b shipping emissions do not include future diversion shipping. Winther et al. (2017) state that Arctic shipping emissions are -7% for SO_2, $+4\%$ for NO_x and -55% for BC in 2012 compared to Winther et al. (2014).

Model simulations for 2050 used Winther et al. (2014) future emission scenarios taking into account growth projections in shipping traffic for a variety of ship types developed by Corbett et al. (2010) and with the addition of fishing emissions. They also include diversion shipping through the Northeast Passage. In the future, reductions in Arctic sea-ice are predicted to open up sea routes which are shorter than traditional routes linking North America or Europe with Asia. Here, 5% of the global total shipping traffic was assumed to be diverted through the Arctic following Corbett et al. (2010). Marelle et al. (2018) evaluated the effects of emission increases from local Arctic sources ($> 60°$N) in summer 2012 and 2050. They showed that shipping emissions from Winther et al. (2014) increase very strongly in summer 2050 (e.g. by 1400% for BC, 1500% for NO_x) due to diversion shipping through the Arctic Ocean. The decrease in Arctic shipping emissions caused by reduced sulphur fuel content is more than compensated for by the projected increase in traffic, and leads to total Arctic shipping SO_2 emissions increasing by 1200% compared to present-day (2012). Future shipping scenarios remain highly uncertain. Here, we focus on examination of potential responses by

using a high growth scenario (HGS) which predicts large increases in Arctic shipping traffic.

2.3. Simulations

To assess the effects of shipping emissions over the Barents Sea and nearby maritime and coastal areas (nested domain in Fig. .1), four simulations were performed: (i) BASE (base case simulation) using the present-day shipping emissions for 2012; (ii) ZERO where present-day shipping emissions were switched off to assess the present-day effect of shipping; (iii) HGS for 2050 using the high growth scenario detailed above and, (iv) HGS-WIDE where diversion shipping in the Arctic was spread over a wider 60 km (3 model grid box) shipping lane, instead of over 20 km (single model grid box) in HGS. The HGS-WIDE scenario explores the sensitivity of model results to dilution of future shipping emissions over a wider area. The coverage of future Arctic shipping lanes is highly uncertain but likely to cover a wider geographic area than considered in this study (Melia et al., 2016).

In order to investigate the impacts of present-day shipping in the Barents Sea region, we compared the BASE and ZERO runs. The difference between HGS or HGS-WIDE scenarios and the BASE run was used to examine the impact of future shipping on O_3, NO_3^-, SO_4^{2-} concentrations and nitrogen (N) and sulphur (S) deposition.

The model version used in this study has already been evaluated against aerosol and ozone observations in the Arctic during summer showing reasonable performance (Raut et al., 2017; Marelle et al., 2017; Law et al., 2017). In the Supplementary Material, results from the nested domain are evaluated against observed concentrations of SO_4^{2-}, NO_3^- and O_3 and

wet and dry deposition fluxes from the European Monitoring and Evaluation Programme (EMEP) network over Europe obtained from EBAS (http://ebas.nilu.no/) at different sites Tustervatn, Mount Zeppelin, Birkenes, Pinega, Janiskoski, Pallas, Oulanka, Esrange (Fig. .1) in summer 2012. Time series and correlation plots between observations and model results for all selected stations illustrate reasonable model performance (Supplementary Material).

3. Results and discussion

3.1. Impacts of shipping on air pollutants in the Barents Sea region

3.1.1. Present-day impacts on pollutant concentrations

The monthly mean mixing ratios of O_3 and NO_x for summer 2012 are shown in Fig. .2.

[Figure 2 about here.]

Figure .2 shows monthly mean surface O_3 concentrations for summer 2012 of around $\sim$ 20 ppbv to 30 ppbv in the Barents Sea region. Lower values in the north of the domain are due to lower NO_x concentrations (< 0.1 ppbv) and efficient removal of O_3 by $O(^1D) + H_2O$ in summer, as well as dry deposition to the ocean. Figure .2 also shows large contributions from present-day shipping of up to 9 ppbv O_3 locally, in particular where NO_x concentrations are low, north of 70°N. Lower O_3 enhancements are found in shipping lanes along the coast of Norway or between northern Norway and Svalbard where half the NO_x is from shipping emissions and reaches 1 ppbv locally. These results suggest that Arctic shipping is already a significant source of O_3

during summer when both shipping emissions and photochemistry are the highest. The enhancements predicted in this study are larger than those reported by Ødemark et al. (2012) ($2-3$ ppbv) or Aksoyoglu et al. (2016) ($<3\%$) using lower shipping NO_x emissions than Winther et al. (2014), but are consistent with results from Marelle et al. (2018), suggesting that 15 to 25% of O_3 is due to Arctic shipping activities over the Norwegian, Barents and Kara Seas (Fig. .1).

[Figure 3 about here.]

Figure .3 shows monthly mean surface summer aerosol concentrations and the impact of present-day shipping emissions. Along the Northeast Passage, average SO_4^{2-} concentrations are $\sim 0.4\mu g\,m^{-3}$ with $2-10\%$ ($\sim 0.04\mu g\,m^{-3}$) from present-day shipping activities spread over a larger area than the shipping tracks. Over land, surface SO_4^{2-} concentrations are also affected by shipping emissions over northern Scandinavia and Russia. The impact of shipping on surface NO_3^- concentrations is larger, ranging from $0.08-0.15\mu g\,m^{-3}$ in the western Barents Sea and reaching $0.2\mu g\,m^{-3}$ along the west coast of Norway (Fig. .3). This represents a $\sim 20\%$ enhancement in NO_3^- due to present-day shipping. Smaller contributions from shipping are found over land, of similar magnitude to SO_4^{2-} ($\sim 0.04\mu g\,m^{-3}$). These results are comparable, but slightly larger, than previous studies. Jonson et al. (2015) estimated increases of the order of $2-5\%$ in SO_4^{2-} due to shipping in the Southern Norwegian coast, an area comparable to this study. Karl et al. (2019b) estimated an average contribution from shipping to $PM_{2.5}$ (including SO_4^{2-}, NO_3^-) in coastal land areas around the Baltic Sea in the range $3.1-5.7\%$ using three different

chemistry transport models. Differences between studies may be ascribed to different regions, some where sulphur and nitrogen emission reduction regulations already apply, but also to differences in model aerosol treatments, in particular with respect to inorganic aerosol formation. Our results suggest that shipping activities could already be having an influence on levels of air pollutants over the Barents Sea region.

3.1.2. Future impacts on pollutant concentrations

Figure .4 shows the contribution of future shipping emissions on O_3, NO_3^- and SO_4^{2-} concentrations in summer 2050. Outside the main shipping lane (Northeast Passage), a large impact on O_3 is found in particular due to the inclusion of diversion shipping in the future scenario (HGS and HGS-WIDE). Enhancements in O_3 mixing ratios up to 5.5 ppbv are predicted in low NO_x regions, especially in the Kara Sea (Fig. .4). Along the diversion route, O_3 may increase or decrease depending on the local chemistry regime (low-NO_x or high-NO_x, as already noted for the present-day). Where NO_x emissions are large, O_3 titration by the reaction with NO occurs along the main shipping lane leading to lower predicted future O_3. Notable differences are found depending on how the diversion route is included in the future simulations. The effect of widening the diversion route (HGS-WIDE) is twofold and highly non-linear. First, the region where O_3 titration occurs north of Norway is spread over a wider area but decreases in O_3 are lower (1 ppbv in HGS-WIDE compared to 5 ppbv in HGS). Second, O_3 production is increased in low NO_x regions in the Kara Sea due to the introduction of diversion shipping NO_x over a wider area in HGS-WIDE. Finally, although local shipping emissions have a local titration effect, diversion emissions as a whole may increase O_3

levels over most of the Arctic since, due to the lifetime of O_3 (several days) in summer, O_3 produced from shipping emissions can be transported away from the shipping lanes. These results highlight the sensitivity of Arctic O_3 to the way in which diversion shipping, in particular, is introduced in models.

[Figure 4 about here.]

Figure .4 also shows differences in NO_3^- and SO_4^{2-} concentrations between the HGS scenario and the BASE simulation. Increased shipping emissions, largely due to traffic diversion, are responsible for moderate increases in SO_4^{2-} concentrations ($\sim +37\%$) relative to the present-day ($0.4\mu g\,m^{-3}$ in the coastal areas (Fig. .3) and up to $0.15\mu g\,m^{-3}$ over the whole domain. This is because HGS SO_2 emissions do not increase by much due to implemented sulphur emission mitigation. In contrast, large increases (by around 100%), in the range $0.5 - 0.7\mu g\,m^{-3}$, are predicted for NO_3^- aerosols in the region of the diversion route. As a consequence, future shipping emissions may lead, on average, to a doubling of NO_3^- concentrations over the Barents Sea region.

3.2. Impacts of shipping on pollutant deposition in the Barents Sea region

3.2.1. Present-day impacts on wet and dry deposition

Figure .5 shows total (wet and dry) N and S deposition from the BASE simulation and the absolute differences between BASE simulation and the ZERO run with emissions switched off for July and August. Here, total N deposition includes wet and dry deposition of NO_3^-, NH_4^+ aerosols, nitric acid (HNO_3), ammonia (NH_3) and minor gaseous N species. Total S deposition includes wet deposition of SO_4^{2-} aerosols, sulphuric acid (H_2SO_4) and dry deposition of SO_2. The model predicts that most of the present-day total N

deposition is over land ($0.6-1.2$ mgN/m^2/day). The amount of N deposited over the ocean is smaller, with an average value of 0.3 mgN/m^2/day and a maximum of 0.7 mgN/m^2/day over the Barents Sea. The contribution from wet deposition fluxes due to present-day shipping presents a spotty distribution because it closely follows modelled precipitation patterns. The largest values are found over the western part of the Barents Sea (0.03 mgN/m^2/day on average, +10% contribution) and reaching 0.05 mgN/m^2/day locally. Dry deposition fluxes due to shipping have a smoother distribution, with values of $\sim$ 0.01 mgN/m^2/day over the Barents Sea (+3% contribution). Higher contributions are estimated along the Norwegian coast ($\sim 0.02-0.03$ mgN/m^2/day, +10%) where NO_x emissions are at maximum. These results suggest that shipping already plays a role in the deposition of nitrogen.

In the BASE simulation, total S deposition in the domain is quite low (0.3 mgS/m^2/day), with nevertheless higher values along the northern coast of Russia and the Timan-Pechora Basin in northern Siberia (Fig. .1) ($0.5-0.7$ mgS/m^2/day). Specific spots over land are due to high local SO_2 emissions in Russia from metal smelters (up to 2 mgS/m^2/day). Shipping has an important effect on dry deposition of pollutants as they emit close to the surface and in the boundary layer, whereas wet deposition is highly non-linear and also sensitive to pollution aloft. Wet deposition of S due to shipping can only be detected along the western coast of Norway ($0.02-0.04$ mgS/m^2/day, +10% contribution). In contrast, dry S deposition due to shipping has considerable influence along the Norwegian coast contributing on average $\sim$ 0.1 mgS/m^2/day ($\sim$ +150%) and, to a lesser extent, along shipping lanes between northern Norway and the Svalbard archipelago ($0.03-0.04$

288 mgS/m^2/day, +10%).

289 [Figure 5 about here.]

290 *3.2.2. Future impacts on pollutant deposition*

291 Figure .6 shows the absolute differences in July-August average dry and
292 wet deposition of N and S between the future scenario (HGS) and the BASE
293 run. The influence of diversion shipping can clearly be seen. An interesting
294 result of this study is that dry and wet N deposition contribute almost equally
295 to absolute enhancements of future N deposition ($\sim$ +10 Gg over the ocean
296 in July-August). Values as high as $0.13 - 0.2$ mgN/m^2/day ($+25 - 50\%$)
297 are estimated for dry N deposition in the proximity of the shipping lanes,
298 but are spread over a larger area, reaching land, and expanding toward the
299 Timan-Pechora Basin and the west Siberian Plain covered by tundra. The
300 distribution of wet N deposition is even more spread out affecting almost
301 similarly (0.15 mgN/m^2/day, +50%) most of the Nordic waters (Norwegian,
302 Barents and Kara Seas) but also the coastal areas of northern Russia and
303 to a lesser extent northern Norway. Over the ocean, we estimate the total
304 amount of N deposited in July-August 2050 to be $\sim$ 56.5 Gg N from all
305 sources. This represents an increase of +22% in deposition due to future
306 shipping compared to present-day. Extrapolation of our estimate to ice-
307 free regions over the entire Arctic Ocean (May to September) would suggest
308 a much larger potential contribution than previous estimates such as that
309 from Lamarque et al. (2013) who estimated annual total future atmospheric
310 N deposition from all sources of $\sim$ 100 Gg/year over the ice-free Arctic Ocean.
311 A recent study by Terhaar et al. (2021) concluded, based on the results of

Lamarque et al. (2013), that present-day atmospheric N deposition is not important compared to other sources like riverine import ($\sim$ 1 Tg/year) and coastal erosion ($\sim$ 1.6 Tg/year). In contrast, our results imply that the future deposition of atmospheric N due to increased shipping emissions in the Arctic may have a substantial effect ecological impact, especially since the shipping lanes coincide with high primary productivity in this nitrogen poor marine ecosystem (Baker et al., 2017; Tuerena et al., 2021).

Future emissions also lead to large increases in dry S deposition fluxes ($\sim$ 1 mgS/m^2/day) in the vicinity of the shipping lanes. This corresponds to an enhancement of +114% of total S deposited over the ocean compared to present-day. Over land, substantial increases in dry S deposition fluxes only occur in hotspots associated with higher future SO_2 emissions due to the energy and industrial sectors in the ECLIPSE inventory. Enhancements in wet S deposition due to future shipping show similar spatial distributions as wet N deposition since they are also linked to simulated clouds and precipitation, but of slightly smaller magnitude ($\sim$ 0.1 mgS/m^2/day). Over the ocean, the total amount of S deposited in July-August 2050 is estimated to be $\sim$ 43 Gg, representing an increase of +37% compared to present-day deposition.

Ozone deposition is also enhanced in the south of the Novaya Zemlya archipelago, along the coastal region of the west Siberian Plain with values reaching 3 mg/m^2/day (+15%, not shown). Future shipping emissions contribute to 21% (5.8 Gg N/month) and 34% (7.3 Gg S/month) to the total amount of N and S deposited over the Ocean in summer 2050. Without a plan to define the Barents Sea region and other Arctic seas as nitrogen or sulphur Emission Control Areas (NECAs/SECAs) in the foreseeable future,

the deposition fluxes of N and S due to shipping will greatly increase in the warming Arctic.

[Figure 6 about here.]

4. Conclusions

The results of our study suggest that Arctic shipping is already affecting atmospheric composition in the Barents Sea region, and in particular ozone and nitrate aerosol concentrations. Using a high growth scenario for future shipping which also includes diversion shipping, substantial increases in ozone are predicted, especially in areas where NO_x concentrations are low. Results are very sensitive to the way in which diversion shipping is included in the model and points to the need for more accurate determination of possible routes along the Northeast Passage and together with high resolution modelling. Increases in ozone and aerosol concentrations, in particular along coastal areas, has implications for background levels of these air pollutants which are damaging to human health. We also predict large total nitrogen deposition over the Barents Sea region due to future shipping based on the high growth scenario. This may be an upper estimate but is nevertheless higher than one prior estimate and suggests that atmospheric nitrogen input to the Arctic Ocean may increase considerably in the future. It may already be important, in contrast to what has already been published. This has implications for marine primary productivity, in particular in the Barents Sea which is a nitrogen-poor in terms of oceanic nutrients. We also predict significant dry sulphur deposition in the vicinity of shipping lanes. Such increases

in deposition of acidic pollutants from shipping emissions may have the potential to increase ocean acidity locally. Deposition of nitrogen and sulphur over coastal areas (forest, tundra) may also affect land-based ecosystems. Finally, ozone deposition is also enhanced along the eastern coasts of the Barents Sea and inland. These findings should be considered in discussions about possible implementation of regulations to limit shipping emissions in the fragile Arctic environment.

Acknowledgments

The authors acknowledge the support of the ICE-ARC programme from the European Union Seventh Framework Programme grant number 603887. Computer analyses benefited from access to IDRIS HPC resources (GENCI allocations A007017141 and A009017141) and the IPSL mesoscale computing center (CICLAD: Calcul Intensif pour le CLimat, l'Atmosphère et la Dynamique).

Competing interests

The authors declare that they have no conflict of interest.

Author statement

Jean-Christophe Raut: Conceptualization, Methodology, Formal analysis, Investigation, Writing, Supervision. **Kathy S. Law:** Conceptualization, Methodology, Formal analysis, Investigation, Writing, Supervision, Funding acquisition. **Tatsuo Onishi:** Software, Validation, Formal analysis,

Data curation, Visualization. **Nikos Daskalakis:** Methodology, Software, Data curation. **Louis Marelle:** Methodology, Resources.

References

AACA, 2017. Summary overview of scientific report detailing the results of the Adaptation Actions for a Changing Arctic (AACA) - Barents regional pilot study. Technical Report. AMAP Secretariat, Gaustadallée 21, N-0349 Oslo, Norway.

Aksoyoglu, S., Baltensperger, U., Prévôt, A.S.H., 2016. Contribution of ship emissions to the concentration and deposition of air pollutants in Europe. Atmospheric Chemistry and Physics 16, 1895–1906. URL: https://www.atmos-chem-phys.net/16/1895/2016/, doi:10.5194/acp-16-1895-2016.

Aliabadi, A.A., Thomas, J.L., Herber, A.B., Staebler, R.M., Leaitch, W.R., Schulz, H., Law, K.S., Marelle, L., Burkart, J., Willis, M.D., Bozem, H., Hoor, P.M., Köllner, F., Schneider, J., Levasseur, M., Abbatt, J.P.D., 2016. Ship emissions measurement in the arctic by plume intercepts of the canadian coast guard icebreaker *Amundsen* from the *Polar 6* aircraft platform. Atmospheric Chemistry and Physics 16, 7899–7916. URL: https://www.atmos-chem-phys.net/16/7899/2016/, doi:10.5194/acp-16-7899-2016.

Baker, A.R., Kanakidou, M., Altieri, K.E., Daskalakis, N., Okin, G.S., Myriokefalitakis, S., Dentener, F., Uematsu, M., Sarin, M.M., Duce, R.A., Galloway, J.N., Keene, W.C., Singh, A., Zamora, L.,

Lamarque, J.F.J.F., Hsu, S.C.S.C., Rohekar, S.S., Prospero, J.M., 2017. Observation- and model-based estimates of particulate dry nitrogen deposition to the oceans. Atmospheric Chemistry and Physics 17, 8189–8210. URL: https://www.atmos-chem-phys.net/17/8189/2017/https://doi.org/10.5194/acp-17-8189-2017, doi:10.5194/acp-17-8189-2017.

Box, J.E., Colgan, W.T., Christensen, T.R., Schmidt, N.M., Lund, M., Parmentier, F.J.W., Brown, R., Bhatt, U.S., Euskirchen, E.S., Romanovsky, V.E., Walsh, J.E., Overland, J.E., Wang, M., Corell, R.W., Meier, W.N., Wouters, B., Mernild, S., Mård, J., Pawlak, J., Olsen, M.S., 2019. Key indicators of arctic climate change: 1971–2017. Environmental Research Letters 14, 045010. URL: https://doi.org/10.1088/1748-9326/aafc1b, doi:10.1088/1748-9326/aafc1b.

Corbett, J.J., Lack, D.A., Winebrake, J.J., Harder, S., Silberman, J.A., Gold, M., 2010. Arctic shipping emissions inventories and future scenarios. Atmospheric Chemistry and Physics 10, 9689–9704. URL: http://www.atmos-chem-phys.net/10/9689/2010/, doi:10.5194/acp-10-9689-2010.

Dalsøren, S.B., Endresen, Ø., Isaksen, I.S.A., Gravir, G., Sørgård, E., 2007. Environmental impacts of the expected increase in sea transportation, with a particular focus on oil and gas scenarios for Norway and northwest Russia. Journal of Geophysical Research: Atmospheres 112. doi:10.1029/2005jd006927.

Duce, R.A., LaRoche, J., Altieri, K., Arrigo, K.R., Baker, A.R., Capone,

D.G., Cornell, S., Dentener, F., Galloway, J., Ganeshram, R.S., Geider, R.J., Jickells, T., Kuypers, M.M., Langlois, R., Liss, P.S., Liu, S.M., Middelburg, J.J., Moore, C.M., Nickovic, S., Oschlies, A., Pedersen, T., Prospero, J., Schlitzer, R., Seitzinger, S., Sorensen, L.L., Uematsu, M., Ulloa, O., Voss, M., Ward, B., Zamora, L., 2008. Impacts of atmospheric anthropogenic nitrogen on the open ocean. Science 320, 893–897. URL: https://science.sciencemag.org/content/320/5878/893, doi:10.1126/science.1150369, arXiv:https://science.sciencemag.org/content/320/5878/893.full.pdf.

Eckhardt, S., Quennehen, B., Olivié, D.J.L., Berntsen, T.K., Cherian, R., Christensen, J.H., Collins, W., Crepinsek, S., Daskalakis, N., Flanner, M., Herber, A., Heyes, C., Hodnebrog, Ø., Huang, L., Kanakidou, M., Klimont, Z., Langner, J., Law, K.S., Lund, M.T., Mahmood, R., Massling, A., Myriokefalitakis, S., Nielsen, I.E., Nøjgaard, J.K., Quaas, J., Quinn, P.K., Raut, J.C., Rumbold, S.T., Schulz, M., Sharma, S., Skeie, R.B., Skov, H., Uttal, T., von Salzen, K., Stohl, A., 2015. Current model capabilities for simulating black carbon and sulfate concentrations in the Arctic atmosphere: a multi-model evaluation using a comprehensive measurement data set. Atmospheric Chemistry and Physics 15, 9413–9433. URL: http://www.atmos-chem-phys.net/15/9413/2015/, doi:10.5194/acp-15-9413-2015.

Fast, J.D., Gustafson, W.I., Easter, R.C., Zaveri, R.A., Barnard, J.C., Chapman, E.G., Grell, G.A., Peckham, S.E., 2006. Evolution of ozone, particulates, and aerosol direct radiative forcing in the vicinity of Houston using

a fully coupled meteorology-chemistry-aerosol model. Journal of Geophysical Research: Atmospheres 111. URL: http://dx.doi.org/10.1029/2005JD006721, doi:10.1029/2005jd006721.

Gong, W., Beagley, S.R., Cousineau, S., Sassi, M., Munoz-Alpizar, R., Ménard, S., Racine, J., Zhang, J., Chen, J., Morrison, H., et al., 2018. Assessing the impact of shipping emissions on air pollution in the canadian arctic and northern regions: current and future modelled scenarios. Atmospheric Chemistry and Physics 18, 16653–16687.

Granier, C., Niemeier, U., Jungclaus, J.H., Emmons, L., Hess, P., Lamarque, J.F., Walters, S., Brasseur, G.P., 2006. Ozone pollution from future ship traffic in the Arctic northern passages. Geophysical Research Letters 33. URL: https://agupubs.onlinelibrary.wiley.com/doi/abs/10.1029/2006GL026180, doi:10.1029/2006GL026180.

Grell, G.A., Peckham, S.E., Schmitz, R., McKeen, S.A., Frost, G., Skamarock, W.C., Eder, B., 2005. Fully coupled "online" chemistry within the WRF model. Atmospheric Environment 39, 6957–6975. doi:10.1016/j.atmosenv.2005.04.027.

Guenther, A., Karl, T., Harley, P., Wiedinmyer, C., Palmer, P.I., Geron, C., 2006. Estimates of global terrestrial isoprene emissions using MEGAN (Model of Emissions of Gases and Aerosols from Nature). Atmospheric Chemistry and Physics 6, 3181–3210. URL: http://www.atmos-chem-phys.net/6/3181/2006/, doi:10.5194/acp-6-3181-2006.

Hassellöv, I.M., Turner, D.R., Lauer, A., Corbett, J.J., 2013. Shipping

contributes to ocean acidification. Geophysical Research Letters 40, 2731–2736. doi:10.1002/grl.50521.

Im, U., Brandt, J., Geels, C., Hansen, K.M., Christensen, J.H., Andersen, M.S., Solazzo, E., Kioutsioukis, I., Alyuz, U., Balzarini, A., Baro, R., Bellasio, R., Bianconi, R., Bieser, J., Colette, A., Curci, G., Farrow, A., Flemming, J., Fraser, A., Jimenez-Guerrero, P., Kitwiroon, N., Liang, C.K., Nopmongcol, U., Pirovano, G., Pozzoli, L., Prank, M., Rose, R., Sokhi, R., Tuccella, P., Unal, A., Vivanco, M.G., West, J., Yarwood, G., Hogrefe, C., Galmarini, S., 2018. Assessment and economic valuation of air pollution impacts on human health over Europe and the United States as calculated by a multi-model ensemble i the framework of AQMEII3. Atmospheric Chemistry and Physics 18, 5967–5989. URL: https://www.atmos-chem-phys.net/18/5967/2018/, doi:10.5194/acp-18-5967-2018.

Jalkanen, J.P., Johansson, L., Kukkonen, J., Brink, A., Kalli, J., Stipa, T., 2012. Extension of an assessment model of ship traffic exhaust emissions for particulate matter and carbon monoxide. Atmospheric Chemistry and Physics 12, 2641–2659. URL: http://www.atmos-chem-phys.net/12/2641/2012/, doi:10.5194/acp-12-2641-2012.

Jiang, X., Wiedinmyer, C., Carlton, A.G., 2012. Aerosols from Fires: An Examination of the Effects on Ozone Photochemistry in the Western United States. Environmental Science & Technology 46, 11878–11886. URL: http://dx.doi.org/10.1021/es301541k, doi:10.1021/es301541k.

Johansson, L., Jalkanen, J.P., Kukkonen, J., 2017. Global assessment of

499 shipping emissions in 2015 on a high spatial and temporal resolution. At-
500 mospheric Environment 167, 403–415.

501 Jonson, J.E., Jalkanen, J.P., Johansson, L., Gauss, M., van der Gon, H.A.C.,
502 2015. Model calculations of the effects of present and future emissions
503 of air pollutants from shipping in the Baltic Sea and the North Sea.
504 Atmospheric Chemistry and Physics 15, 783–798. URL: https://www.
505 atmos-chem-phys.net/15/783/2015/, doi:10.5194/acp-15-783-2015.

506 Karl, M., Bieser, J., Geyer, B., Matthias, V., Jalkanen, J.P., Johansson, L.,
507 Fridell, E., 2019a. Impact of a nitrogen emission control area (neca) on
508 the future air quality and nitrogen deposition to seawater in the baltic sea
509 region. Atmospheric Chemistry and Physics 19, 1721–1752.

510 Karl, M., Jonson, J.E., Uppstu, A., Aulinger, A., Prank, M., Sofiev, M.,
511 Jalkanen, J.P., Johansson, L., Quante, M., Matthias, V., 2019b. Effects of
512 ship emissions on air quality in the baltic sea region simulated with three
513 different chemistry transport models. Atmospheric Chemistry and Physics
514 19, 7019–7053.

515 Klimont, Z., Kupiainen, K., Heyes, C., Purohit, P., Cofala, J., Rafaj, P.,
516 Borken-Kleefeld, J., Schöpp, W., 2017. Global anthropogenic emissions of
517 particulate matter including black carbon. Atmospheric Chemistry and
518 Physics 17, 8681–8723.

519 Lamarque, J.F., Dentener, F., McConnell, J., Ro, C.U., Shaw, M., Vet, R.,
520 Bergmann, D., Cameron-Smith, P., Dalsoren, S., Doherty, R., et al., 2013.
521 Multi-model mean nitrogen and sulfur deposition from the atmospheric

chemistry and climate model intercomparison project (accmip): evaluation of historical and projected future changes. Atmospheric Chemistry and Physics 13, 7997–8018.

Law, K.S., Roiger, A., Thomas, J.L., Marelle, L., Raut, J.C., Dalsøren, S., Fuglestvedt, J., Tuccella, P., Weinzierl, B., Schlager, H., 2017. Local arctic air pollution: Sources and impacts. Ambio 46, 453–463.

Marelle, L., Raut, J.C., Law, K.S., Berg, L.K., Fast, J.D., Easter, R.C., Shrivastava, M., Thomas, J.L., 2017. Improvements to the WRF-Chem 3.5.1 model for quasi-hemispheric simulations of aerosols and ozone in the Arctic. Geoscientific Model Development 10, 3661–3677. URL: https://www.geosci-model-dev.net/10/3661/2017/, doi:10.5194/gmd-10-3661-2017.

Marelle, L., Raut, J.C., Law, K.S., Duclaux, O., 2018. Current and future arctic aerosols and ozone from remote emissions and emerging local sources—modeled source contributions and radiative effects. Journal of Geophysical Research: Atmospheres 123, 12–942.

Marelle, L., Raut, J.C., Thomas, J.L., Law, K.S., Quennehen, B., Ancellet, G., Pelon, J., Schwarzenboeck, A., Fast, J.D., 2015. Transport of anthropogenic and biomass burning aerosols from Europe to the Arctic during spring 2008. Atmospheric Chemistry and Physics 15, 3831–3850. doi:10.5194/acp-15-3831-2015.

Marelle, L., Thomas, J.L., Raut, J.C., Law, K.S., Jalkanen, J.P., Johansson, L., Roiger, A., Schlager, H., Kim, J., Reiter, A., Weinzierl, B., 2016. Air

quality and radiative impacts of Arctic shipping emissions in the summertime in northern Norway: from the local to the regional scale. Atmospheric Chemistry and Physics 16, 2359–2379. doi:10.5194/acp-16-2359-2016.

Melia, N., Haines, K., Hawkins, E., 2016. Sea ice decline and 21st century trans-arctic shipping routes. Geophysical Research Letters 43, 9720–9728.

Mills, G., Sharps, K., Simpson, D., Pleijel, H., Broberg, M., Uddling, J., Jaramillo, F., Davies, W.J., Dentener, F., Van den Berg, M., et al., 2018. Ozone pollution will compromise efforts to increase global wheat production. Global Change Biology 24, 3560–3574.

Mudryk, L.R., Dawson, J., Howell, S.E., Derksen, C., Zagon, T.A., Brady, M., 2021. Impact of 1, 2 and 4°C of global warming on ship navigation in the Canadian Arctic. Nature Climate Change 11, 673–679.

Nunes, R., Alvim-Ferraz, M., Martins, F., Sousa, S., 2017. The activity-based methodology to assess ship emissions-a review. Environmental pollution 231, 87–103.

Pörtner, H.O., Roberts, D., Masson-Delmotte, V., Zhai, P., Tignor, M., Poloczanska, E., Mintenbeck, K., Alegría, A., Nicolai, M., Okem, A., Petzold, J., Rama, B., Weyer, N.M., 2019. Summary for Policymakers. IPCC Special Report on the Ocean and Cryosphere in a Changing Climate.

Randelhoff, A., Holding, J., Janout, M., Sejr, M.K., Babin, M., Tremblay, J.É., Alkire, M.B., 2020. Pan-arctic ocean primary production constrained by turbulent nitrate fluxes. Frontiers in Marine Science 7. doi:https://doi.org/10.3389/fmars.2020.00150.

Raut, J.C., Marelle, L., Fast, J.D., Thomas, J.L., Weinzierl, B., Law, K.S., Berg, L.K., Roiger, A., Easter, R.C., Heimerl, K., Onishi, T., Delanoë, J., Schlager, H., 2017. Cross-polar transport and scavenging of siberian aerosols containing black carbon during the 2012 access summer campaign. Atmospheric Chemistry and Physics 17, 10969–10995.

Schmale, J., Arnold, S.R., Law, K.S., Thorp, T., Anenberg, S., Simpson, W.R., Mao, J., Pratt, K.A., 2018. Local arctic air pollution: A neglected but serious problem. Earth's Future 6, 1385–1412. URL: https://agupubs.onlinelibrary.wiley.com/doi/abs/10.1029/2018EF000952, doi:10.1029/2018EF000952, arXiv:https://agupubs.onlinelibrary.wiley.com/doi/pdf/10.1029/2018EF000952.

Silber, G.K., Adams, J.D., 2019. Vessel operations in the arctic, 2015–2017. Frontiers in Marine Science 6, 573.

Smedsrud, L.H., Esau, I., Ingvaldsen, R.B., Eldevik, T., Haugan, P.M., Li, C., Lien, V.S., Olsen, A., Omar, A.M., Otterå, O.H., et al., 2013. The role of the barents sea in the arctic climate system. Reviews of Geophysics 51, 415–449.

Stephenson, S.R., Wang, W., Zender, C.S., Wang, H., Davis, S.J., Rasch, P.J., 2018. Climatic responses to future trans-arctic shipping. Geophysical Research Letters 45, 9898–9908. URL: https://agupubs.onlinelibrary.wiley.com/doi/abs/10.1029/2018GL078969, doi:https://doi.org/10.1029/2018GL078969, arXiv:https://agupubs.onlinelibrary.wiley.com/doi/pdf/10.1029/2018GL078969.

Stohl, A., Aamaas, B., Amann, M., Baker, L.H., Bellouin, N., Berntsen, T.K., Boucher, O., Cherian, R., Collins, W., Daskalakis, N., Dusinska, M., Eckhardt, S., Fuglestvedt, J.S., Harju, M., Heyes, C., Hodnebrog, Ø., Hao, J., Im, U., Kanakidou, M., Klimont, Z., Kupiainen, K., Law, K.S., Lund, M.T., Maas, R., MacIntosh, C.R., Myhre, G., Myriokefalitakis, S., Olivié, D., Quaas, J., Quennehen, B., Raut, J.C., Rumbold, S.T., Samset, B.H., Schulz, M., Seland, Ø., Shine, K.P., Skeie, R.B., Wang, S., Yttri, K.E., Zhu, T., 2015. Evaluating the climate and air quality impacts of short-lived pollutants. Atmospheric Chemistry and Physics 15, 10529–10566. URL: http://www.atmos-chem-phys.net/15/10529/2015/, doi:10.5194/acp-15-10529-2015.

Terhaar, J., Lauerwald, R., Regnier, P., Gruber, N., Bopp, L., 2021. Around one third of current arctic ocean primary production sustained by rivers and coastal erosion. Nature communications 12, 1–10.

Tuerena, R.E., Hopkins, J., Ganeshram, R.S., Norman, L., de la Vega, C., Jeffreys, R., Mahaffey, C., 2021. Nitrate assimilation and regeneration in the barents sea: insights from nitrate isotopes. Biogeosciences 18, 637–653. URL: https://bg.copernicus.org/articles/18/637/2021/, doi:10.5194/bg-18-637-2021.

van Vuuren, D.P., Edmonds, J., Kainuma, M., Riahi, K., Thomson, A., Hibbard, K., Hurtt, G.C., Kram, T., Krey, V., Lamarque, J.F., Masui, T., Meinshausen, M., Nakicenovic, N., Smith, S.J., Rose, S.K., 2011. The representative concentration pathways: an overview. Climatic Change 109,

5. URL: https://doi.org/10.1007/s10584-011-0148-z, doi:10.1007/s10584-011-0148-z.

Wiedinmyer, C., Akagi, S.K., Yokelson, R.J., Emmons, L.K., Al-Saadi, J.A., Orlando, J.J., Soja, A.J., 2011. The Fire INventory from NCAR (FINN): a high resolution global model to estimate the emissions from open burning. Geoscientific Model Development 4, 625–641. URL: http://www.geosci-model-dev.net/4/625/2011/, doi:10.5194/gmd-4-625-2011.

Winther, M., Christensen, J., Angelidis, I., Ravn, E., 2017. Emissions from shipping in the Arctic from 2012-2016 and emission projections for 2020, 2030 and 2050. Technical Report. Aarhus University, Danish Centre for Environment and Energy. URL: http://dce2.au.dk/pub/SR252.pdf.

Winther, M., Christensen, J.H., Plejdrup, M.S., Ravn, E.S., Eriksson, Ó.F., Kristensen, H.O., 2014. Emission inventories for ships in the arctic based on satellite sampled AIS data. Atmospheric Environment 91, 1–14. doi:10.1016/j.atmosenv.2014.03.006.

Ødemark, K., Dalsøren, S.B., Samset, B.H., Berntsen, T.K., Fuglestvedt, J.S., Myhre, G., 2012. Short-lived climate forcers from current shipping and petroleum activities in the arctic. Atmospheric Chemistry and Physics 12, 1979–1993. URL: http://www.atmos-chem-phys.net/12/1979/2012/, doi:10.5194/acp-12-1979-2012.

List of Figures

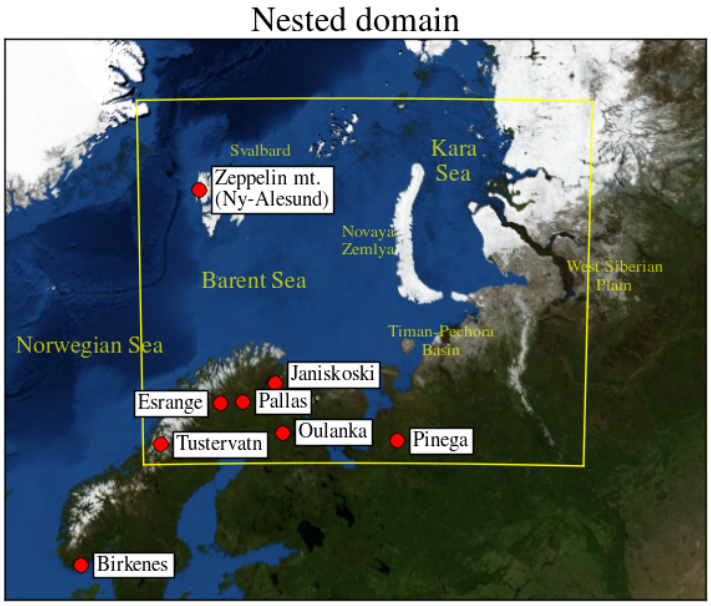

Figure .1: Domains used in the WRF-Chem simulations. The large domain covers most of the Northern Hemisphere in a polar stereographic grid, and the nested domain is centered on the Barents Sea region. Stations used for model evaluation, as well as seas and land regions referred to in the text are also reported on the map.

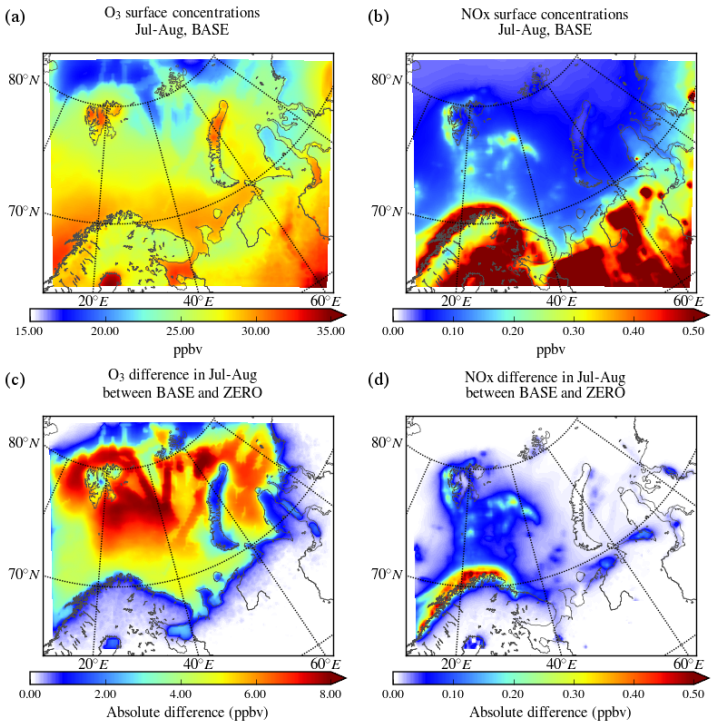

Figure .2: Monthly mean O_3 (a) and NO_x (b) mixing ratios simulated for July-August 2012 (BASE run) and the contribution of present-day shipping (BASE - ZERO) on O_3 (c) and NO_x (d) mixing ratios (in ppbv).

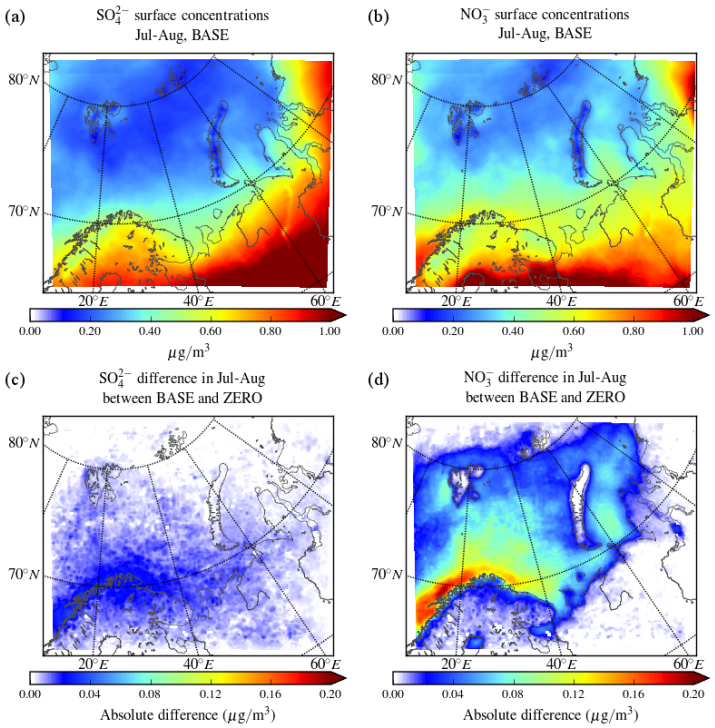

Figure .3: Monthly mean sulphate (a) and nitrate (b) aerosol concentrations predicted by the model for July-August 2012 (BASE run) and absolute differences in present-day sulphate (b) and nitrate (d) concentrations between simulations with (BASE) and without (ZERO) shipping emissions (in $\mu g\,m^{-3}$).

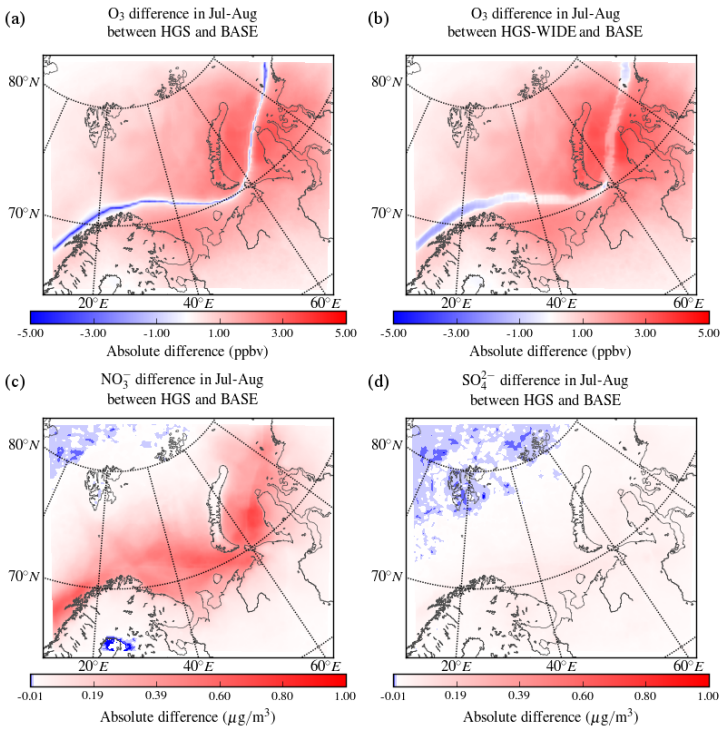

Figure .4: Absolute differences in monthly mean surface O_3 mixing ratios (in ppbv) (a), nitrate aerosol concentrations (in $\mu g\,m^{-3}$) (c) and sulphate aerosol concentrations (in $\mu g\,m^{-3}$) (d) between the HGS scenario and the BASE run. Panel (b) shows the absolute difference in monthly mean surface O_3 mixing ratios between the HGS-WIDE scenario and the BASE run.

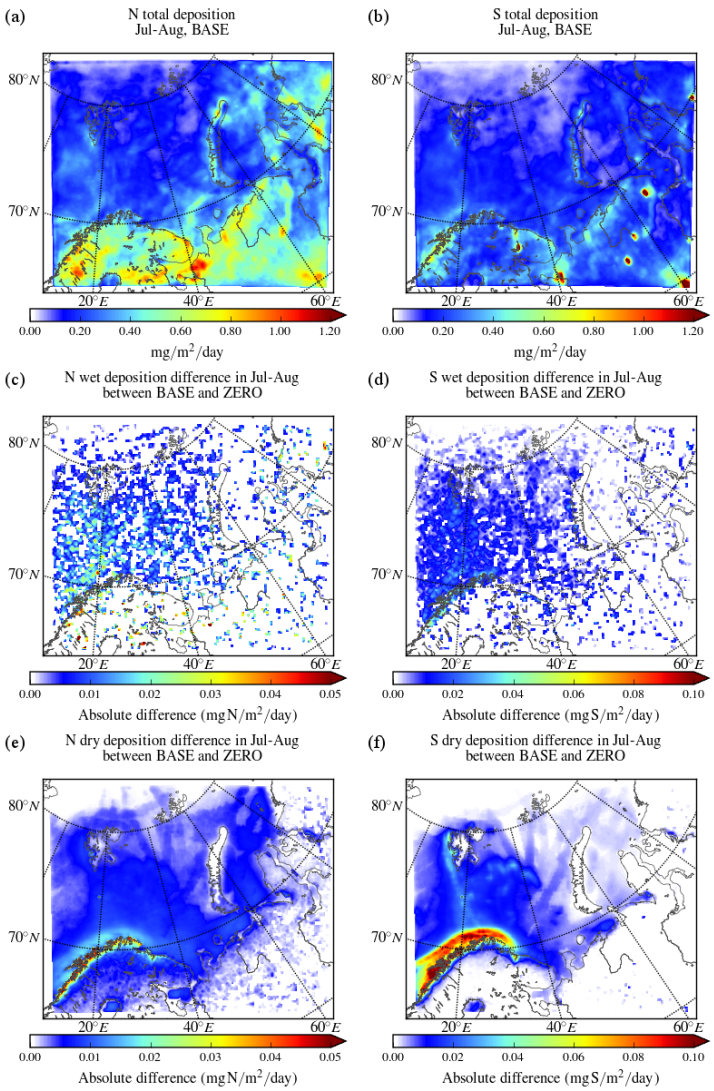

Figure .5: Monthly mean deposition fluxes of total nitrogen (in mgN/m^2/day) (a) and total sulphur (mgS/m^2/day) (b) simulated for July-August 2012 and the contribution of present-day shipping to wet (c,d) and dry (e,f) deposition fluxes of total nitrogen (c,e) and total sulphur (d,f) from differences between simulations with (BASE) and without (ZERO) shipping emissions.

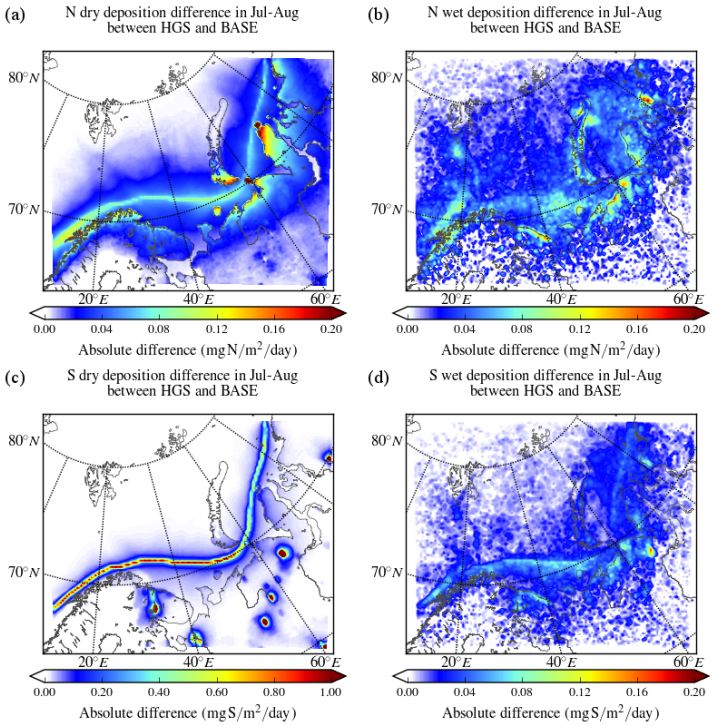

Figure .6: Absolute differences in monthly mean dry (a,c) and wet (b,d) deposition fluxes of total nitrogen (in mgN/m^2/day) (a,b) and total sulphur (in mgS/m^2/day) (c,d) between the HGS scenario and the BASE run.